Electronic Supplementary Material (ESI) for Polymer Chemistry.

Supporting Information

Thermo-responsive 3D-printed Polyrotaxane Monolith

Qianming Lin, Miao Tang and Chenfeng Ke

Department of Chemistry, Dartmouth College, 6128 Burke Laboratory, Hanover, New Hampshire, 03755, United States

Table of Contents

S1. General Information and Synthesis S1

S2. Characterizations S7

S3. 3D Printing and Thermal Responsive Investigation. S14

S4. References S16

S1. General Information and Synthesis

All reagents were purchased from commercial suppliers and used as received without further purifications. α-Cyclodextrin was generously gifted by Wacker Chemical Corporation. Nuclear magnetic resonance (NMR) spectra were recorded on Bruker Ascend 600 or 500 NMR spectrometers. White-light optical microscope images were recorded using AmScope SM-1TSW2 stereomicroscope, and other images were recorded using a regular camera.

3D-printed polyrotaxane monoliths (PMs) were prepared following our established method, and used as the starting material for post-printing methylations.[1,2]

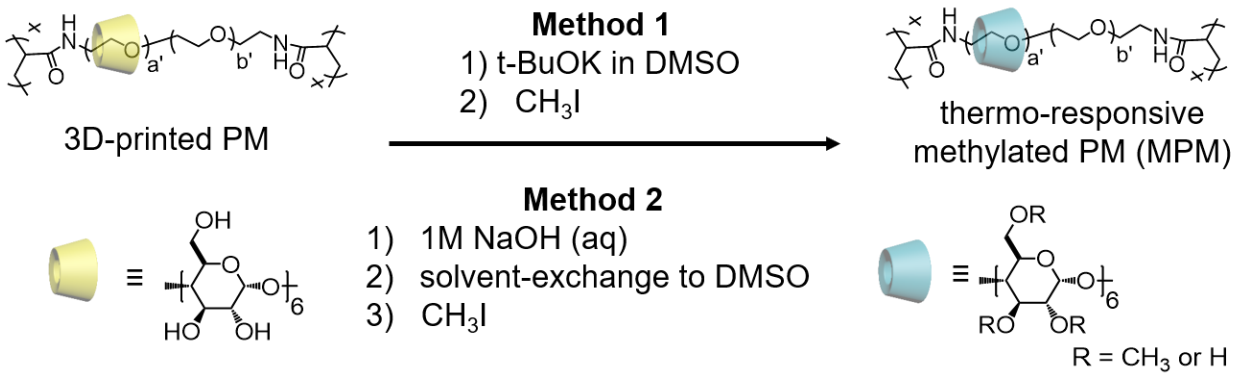

Figure S1. Post-printing methylation of polyrotaxane monoliths.

Methylated polyrotaxane monolith (MPM): Post-printing methylation was conducted in an Erlenmeyer flask on an orbital shaker to protect the macroscale shape of the 3D-printed PM.

Method 1: A PM hydrogel (wet weight = 1.2 g, 5.33×10^{-5} mol α-CD in the monolith) was immersed in anhydrous DMSO (20 mL) in an Erlenmeyer flask, and the reaction was shaken at a speed of 150 rpm for 2 h. The opaque monolith turned transparent, indicating the interruption of hydrogen bonding interactions between α-CDs. Fresh DMSO was used exchange the solvent for three times. A t-BuOK DMSO solution (20 mL, see Table S1) was added and the reaction was shaken for 12 h. The transparent monolith turned opaque and its size reduce significantly. A methyl iodide DMSO solution (0.75 – 32 equiv. to -OH of α-CD) was introduced to the reaction after deprotonation. The reaction was shaken for another 24 h and quenched by an excess of water. The obtained methylated polyrotaxane monoliths (MPMs) were washed using extensive distilled water. The MPM hydrogels were lyophilized for NMR analysis.

Method 2: A PM hydrogel (wet weight = 1.2 g, 5.33×10^{-5} mol α-CD in the monolith) was immersed in 1 M NaOH aqueous solution (20 mL) in an Erlenmeyer flask, and the reaction was shaken at a speed of 150 rpm for 2 h. The opaque monolith turned transparent, indicating an extensive deprotonation of the hydroxyl groups of CDs in the monolith. The deprotonated monolith was collected and washed by DMSO (5 mL × 2) before it was immersed in a fresh DMSO

(20 mL). During the solvent exchange process, the transparent hydrogel turned opaque in the DMSO and its size shrank significantly. After 12 h, the solvent was decanted carefully, and the reaction was recharged with a methyl iodide DMSO solution (20 mL, see Table S2). The opaque monolith gradually turned transparent. The reaction was shaken for another 24 h until the monolith turned completely transparent, and an excess of water was added to quench the reaction. The obtained MPM was washed water and lyophilized for NMR analysis.

Hydrolysis of PM and MPMs: In order to quantitatively measure the number of CDs threaded on PEG in the PM and MPMs, and calculating the methylation degree of the α-CDs in MPMs, lyophilized PM and MPMs were hydrolyzed in DCl solutions for ^{1}H NMR analysis. Generally, a lyophilized monolith (~ 20 mg) was added to DCl (500 µL, 10 % or 20 % v/v in D_2O) in a NMR tube. The reaction was heated to 80 °C until the monolith was completely dissolved. The reaction was cooled to room temperature before the ^{1}H NMR experiment.

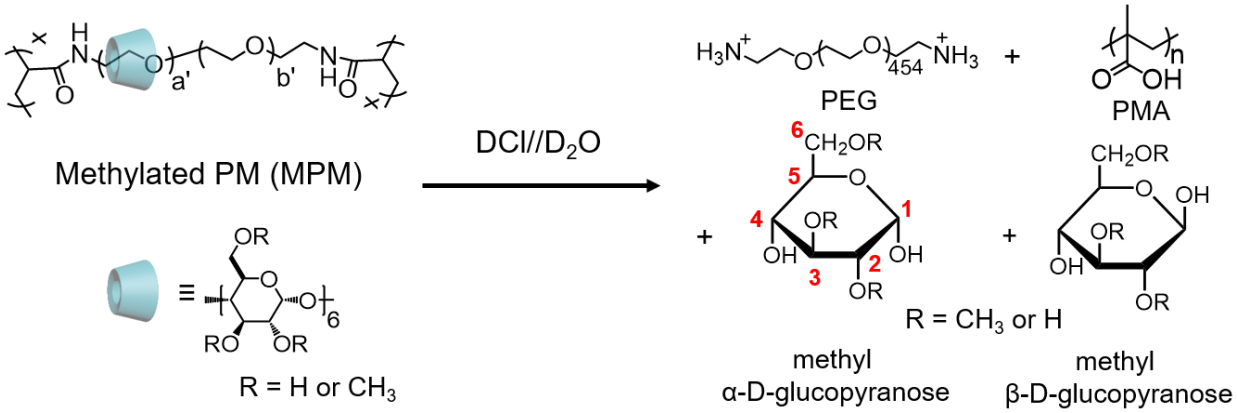

Figure S2. Hydrolysis of MPM in DCl/D_2O (10 % or 20 % v/v).

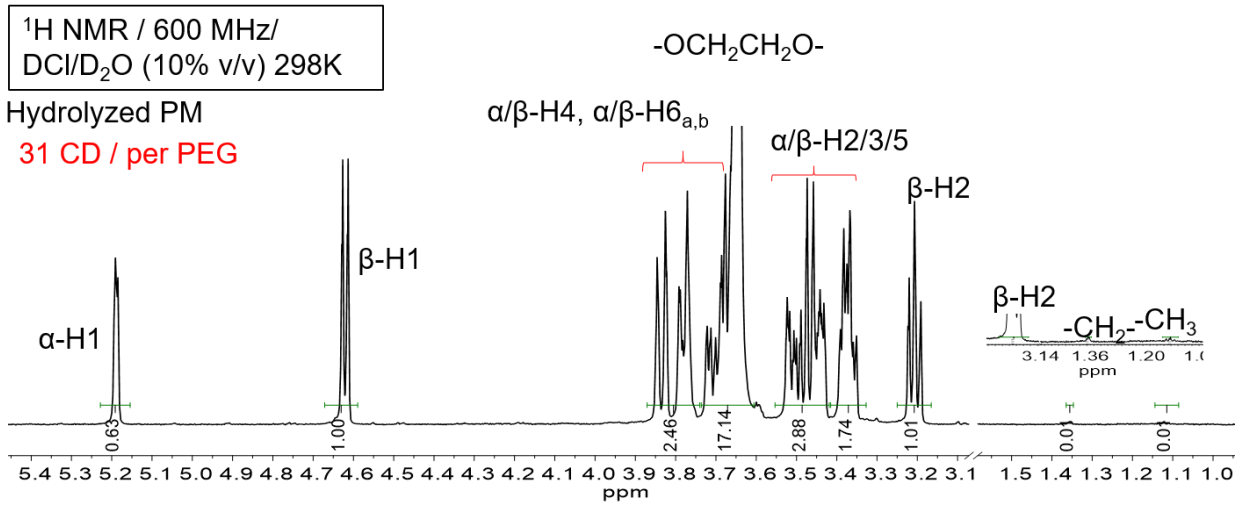

Figure S3. ^{1}H NMR spectrum of hydrolyzed PM in DCl/D_2O (10 % v/v) recorded at 298 K.

Table S1. Number of CDs per PEG, and the calculated methylation degrees (MDs) of MPM at various CH_3I feeding ratios in method 1.

trail 1				trial 2			trial 3		
fed [t-BuOK]: [MeI]: $[(OH)_{CD}]$		CDs per PEG	MD (%)	fed [t-BuOK]: [MeI]: $[(OH)_{CD}]$	CDs per PEG	MD (%)	fed [t-BuOK]: [MeI]: $[(OH)_{CD}]$	CDs per PEG	MD (%)
PM	0	34	0	0	19	0	0	31	0
MPM	2: 2: 1	32	36	0.75: 0.75: 1	19	20	2: 2: 1	40	2
	4: 4: 1	18	32	1.5: 1.5 :1	21	22	4: 4: 1	35	<1
	8: 8: 1	21	21	3: 3: 1	20	50	8: 8: 1	31	<1
				4.5: 4.5: 4.5	19	52	16: 16: 1	31	<1
				6: 6: 6	19	57	32: 32: 1	30	<1

Table S2. Number of CDs per PEG, and the calculated MDs of MPM at various CH_3I feeding ratios in method 2.

trails		1		2		3	
fed [MeI] : $[(OH)_{CD}]$		CDs per PEG	MD (%)	CDs per PEG	MD (%)	CDs per PEG	MD (%)
PM	0	35	0	33	0	33	0
MPM	2: 1	30	55	31	53	34	47
	4: 1	30	78	31	76	30	79
	8: 1	31	82	32	92	31	78
	16: 1	34	90	32	93	31	93
	32: 1	35	90	32	92	30	86

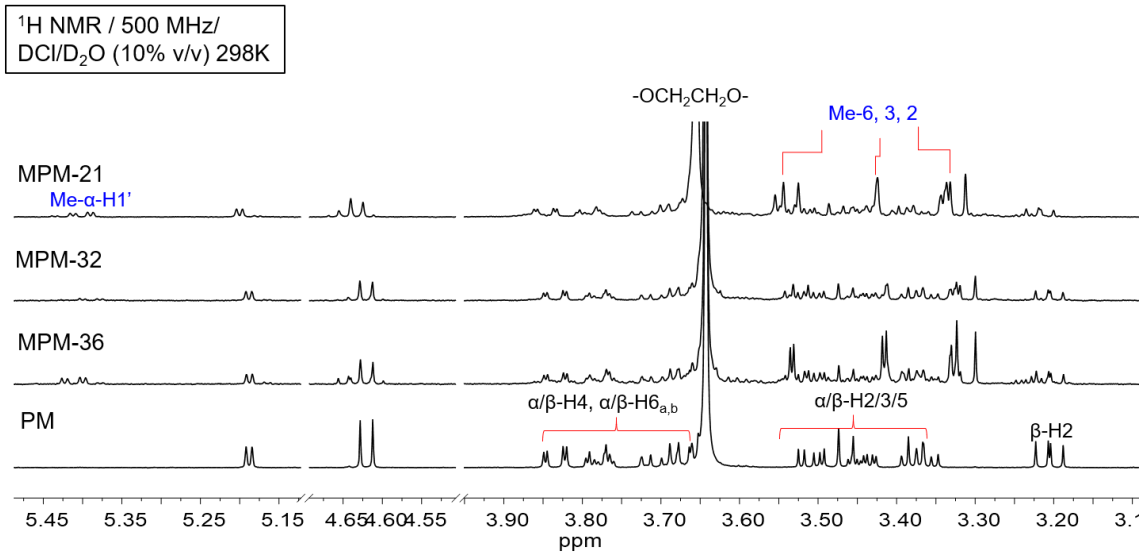

Figure S4. ^{1}H NMR spectra of hydrolyzed MPM (trial 1 in **Table. S1**) in DCl/D_2O (20 % v/v) at 298 K.

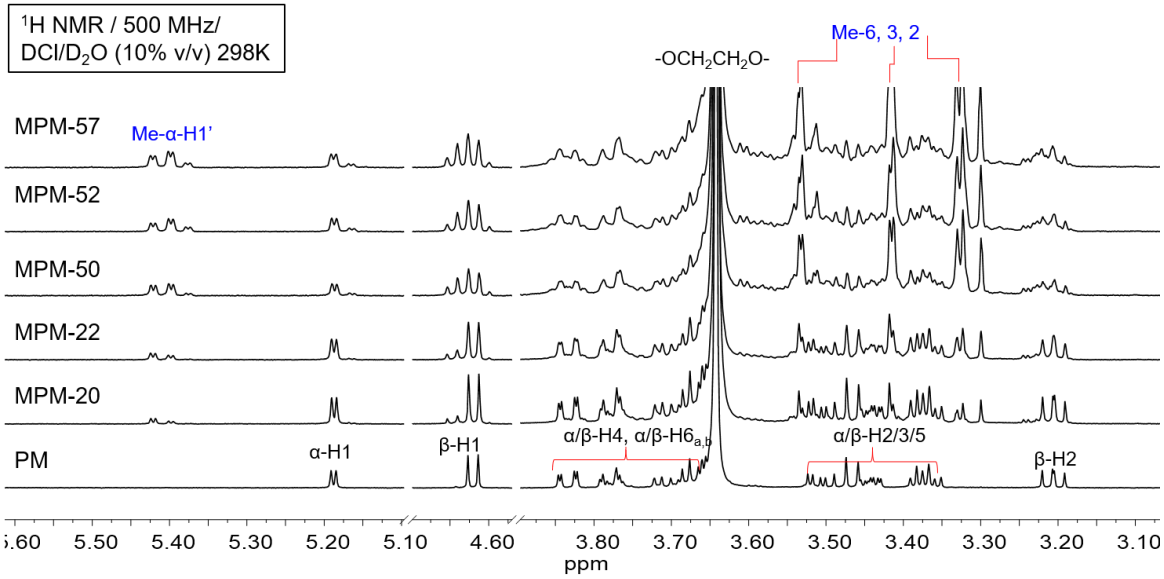

Figure S5. ^{1}H NMR spectra of hydrolyzed MPM (trial 2 in **Table. S1**) in DCl/D_2O (20 % v/v) at 298 K.

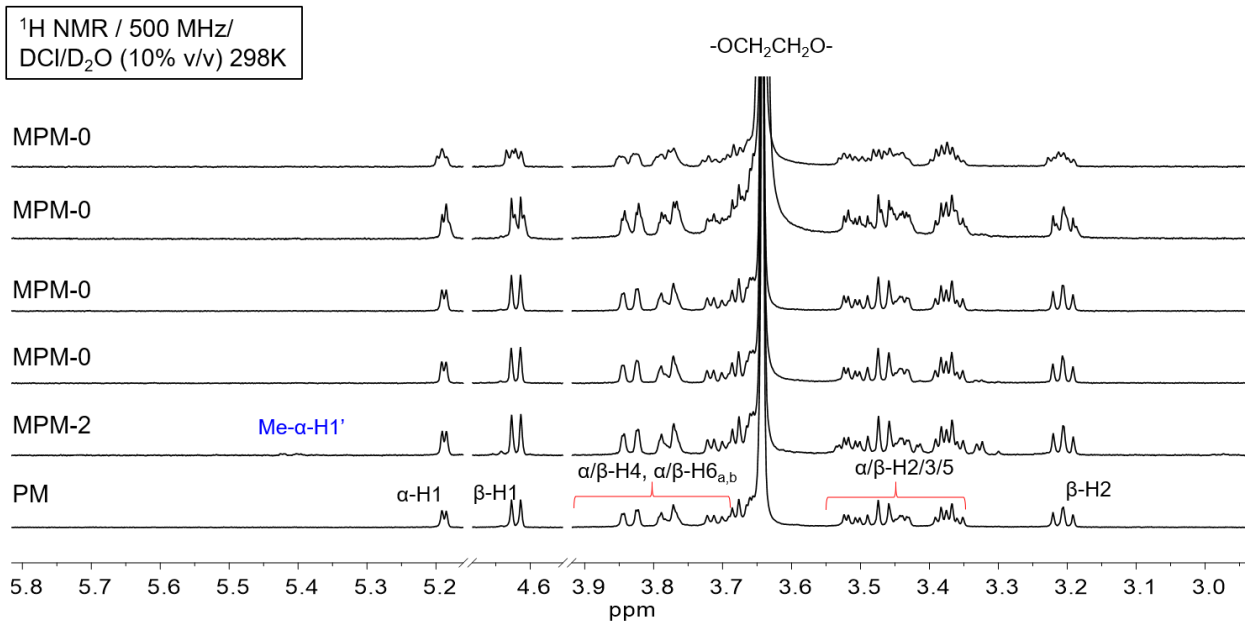

Figure S6. ^{1}H NMR spectra of hydrolyzed MPM (trial 3 in **Table. S1**) in DCl/D_2O (20 % v/v) at 298 K.

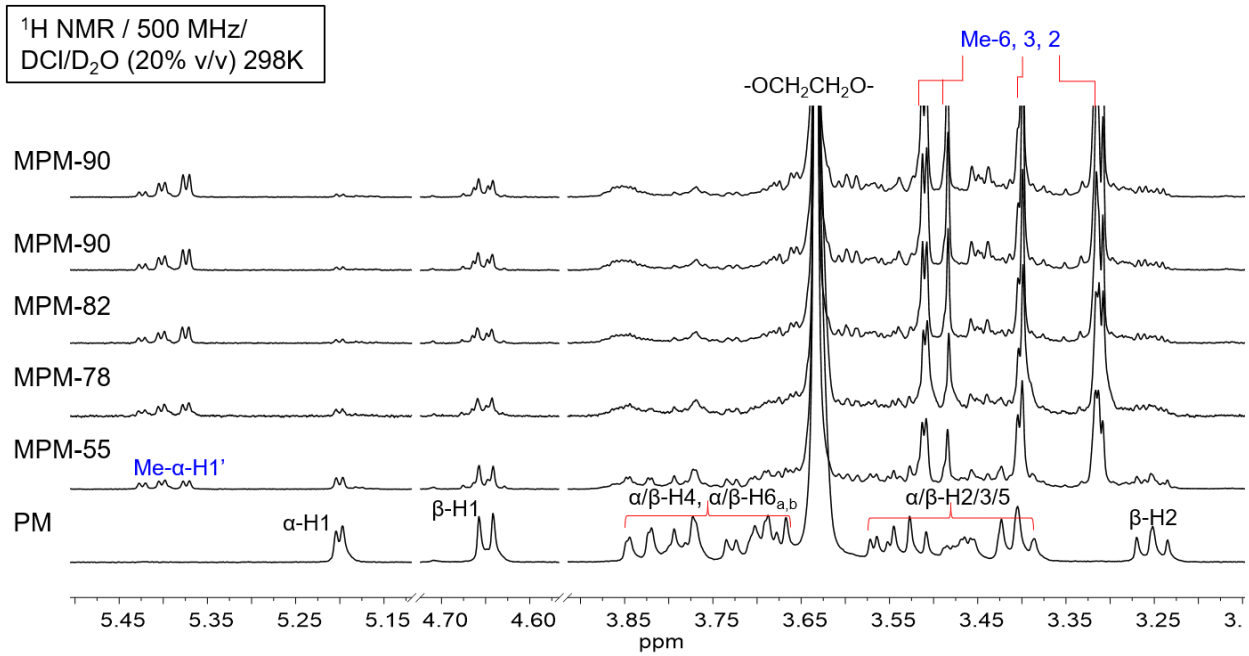

Figure S7. ^{1}H NMR spectra of hydrolyzed MPM (trial 1 in **Table. S2**) in DCl/D_2O (20 % v/v) at 298 K.

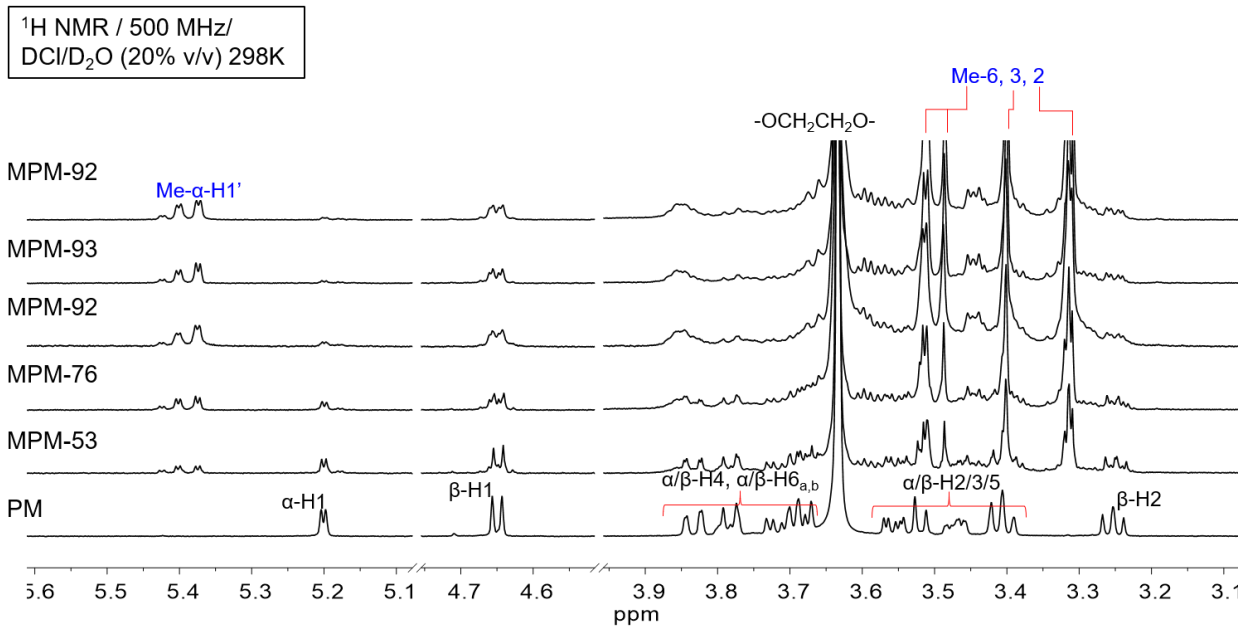

Figure S8. ^{1}H NMR spectra of hydrolyzed MPM (trial 2 in **Table. S1**) in DCl/D_2O (20 % v/v) at 298 K.

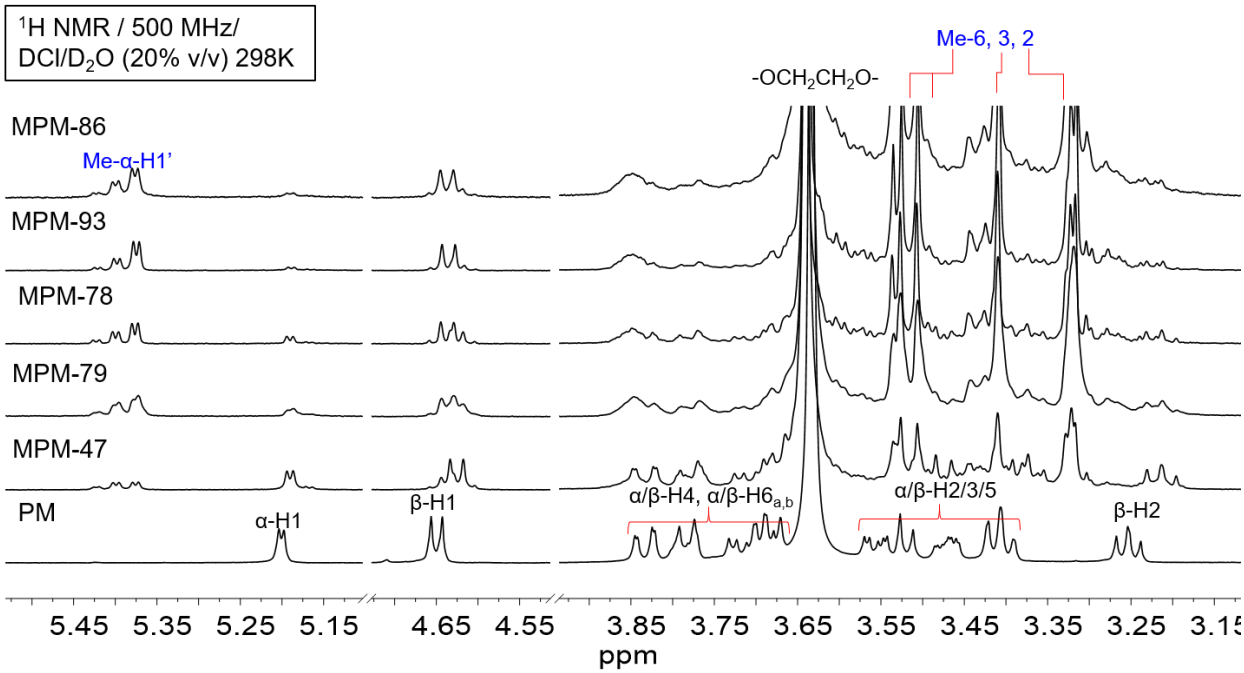

Figure S9. ^{1}H NMR spectra of hydrolyzed MPM (trial 3 in **Table.** S1) in DCl/D_2O (20 % v/v) at 298 K.

S2. Characterizations

Rheological investigation of PM. PM^-/Na^+ hydrogels and DMSO gels were prepare by soaking PM hydrogel in 1 M NaOH, and then solvent exchanged to DMSO, respectively. The hydrogels were subjected to rheological investigations. Frequency-dependent elastic moduli of these gels were scanned between 1 and 100 $rad \cdot s^{-1}$ with a strain of 0.05 % at 25 ºC.

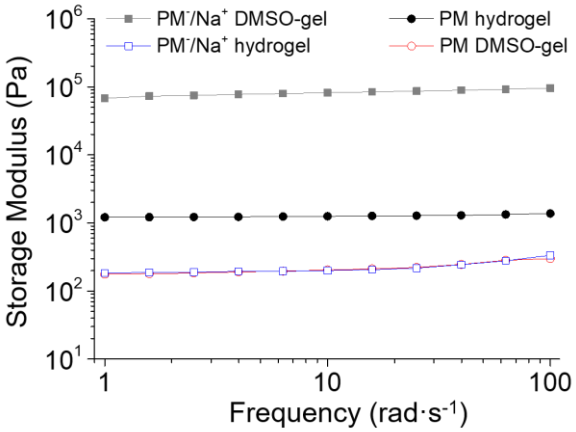

Figure S10. Frequency-dependent elastic moduli of PM^-/Na^+ DMSO-gel, PM hydrogel, PM^-/Na^+ hydrogel and PM DMSO-gel.

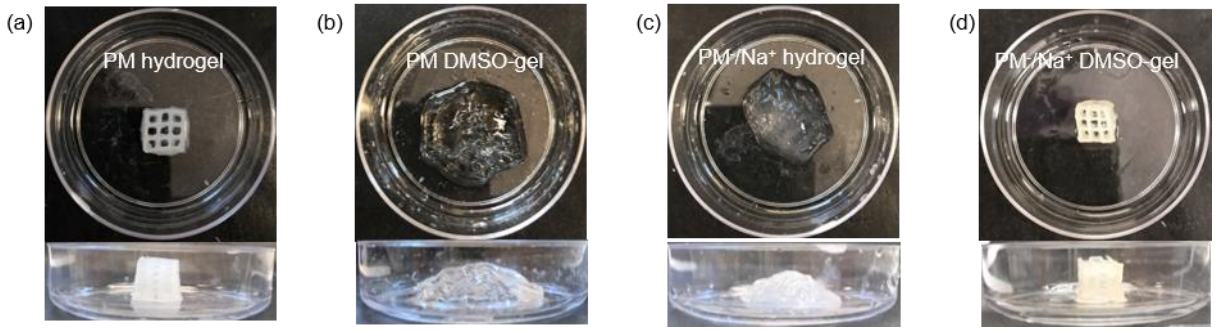

Figure S11. Images of (a) PM hydrogel and (b) DMSO-gel, (c) deprotonated PM^-/Na^+ hydrogel and (d) PM^-/Na^+ DMSO-gel.

Frequency-sweep moduli measurements of MPMs. In order to keep the hydrogels with a constant swelling ratio, MPM hydrogels were soaked in water at 4 ºC for 72 h, then heated to 90 ºC. The solvent was decanted, and the hydrogels were cooled down to 4 ºC. During the measurement, elastic and loss modulus were monitored with a strain of 0.05 % at 4 ºC. The frequency scans from 1 to 100 $rad \cdot s^{-1}$.

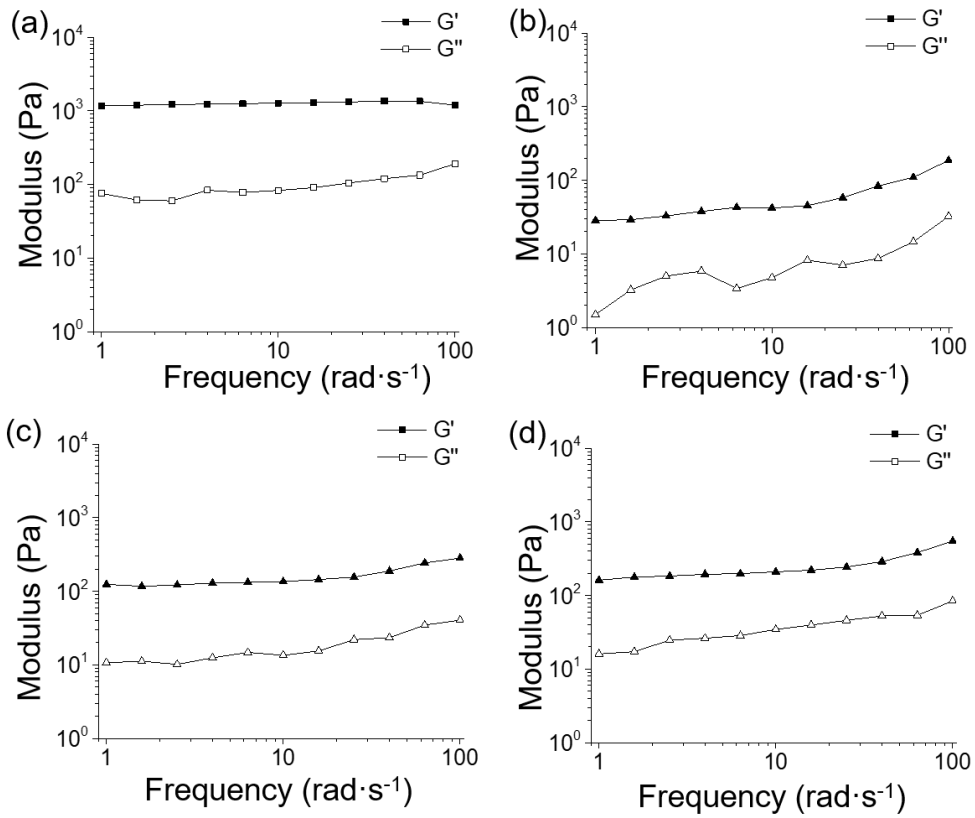

Figure S12. Frequency sweep of (a) PM, (b) MPM-52, (c) MPM-78 and (d) MPM-92, recorded at 4 °C, respectively.

Temperature-sweep moduli measurements of MPMs. The elastic moduli of PM and MPMs were monitored with a frequency of 1 rad^{-1} and a strain of 0.05 %. The temperature-sweep measurement contains a heating step from 4 °C to 85 °C and a cooling step from 85 °C to 4 °C. The scanning rate was set as 3 °C per minute with an equilibrium time of 60 s for each temperature measurement. The heating-cooling cycles were performed three times.

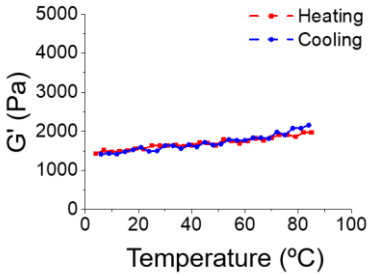

Figure S13. Elastic moduli of PM-52 (4 °C → 85 °C → 4°C).

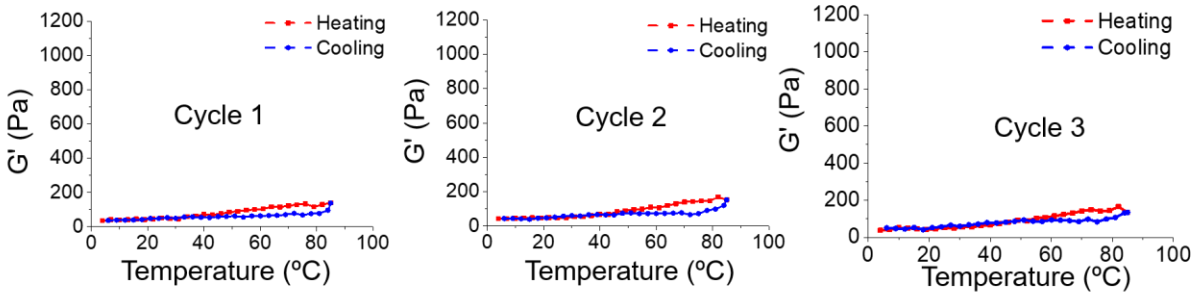

Figure S14. Elastic moduli of MPM-52 (4 ºC → 85 ºC → 4 ºC) in three cycles.

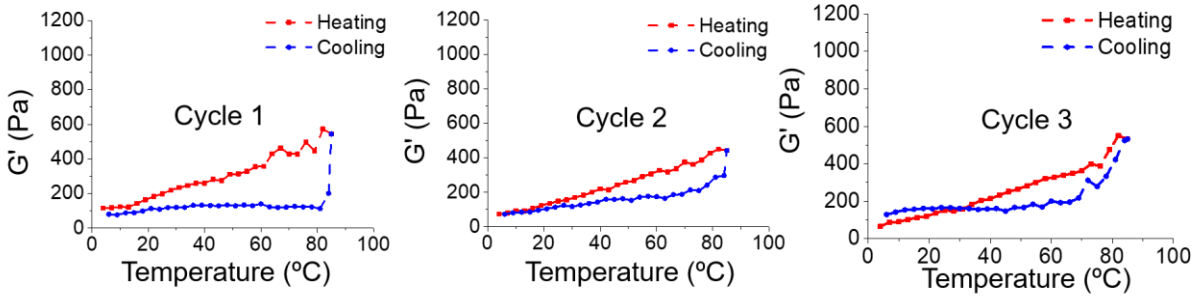

Figure S15. Elastic moduli of MPM-78 (4 ºC → 85 ºC → 4 ºC) in three cycles.

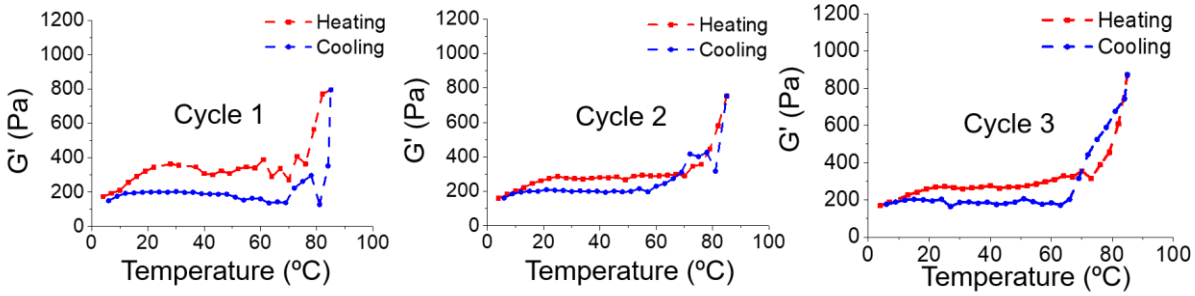

Figure S16. Elastic moduli of MPM-92 (4 ºC → 85 ºC → 4 ºC) in three cycles.

Differential scanning calorimeter (DSC) characterization. PM and MPM hydrogels were stored in water at 4 ºC before measurement at their fully swollen states. These hydrogels (~ 10 mg) were sealed in an aluminum pan. H_2O (10 uL) was used as the reference for each measurement. The scanning range is set between 4 ºC and 90 ºC, with a 10 ºC/min heating ramp. Isothermal states at 4 ºC and 90 ºC were maintained for 5 min.

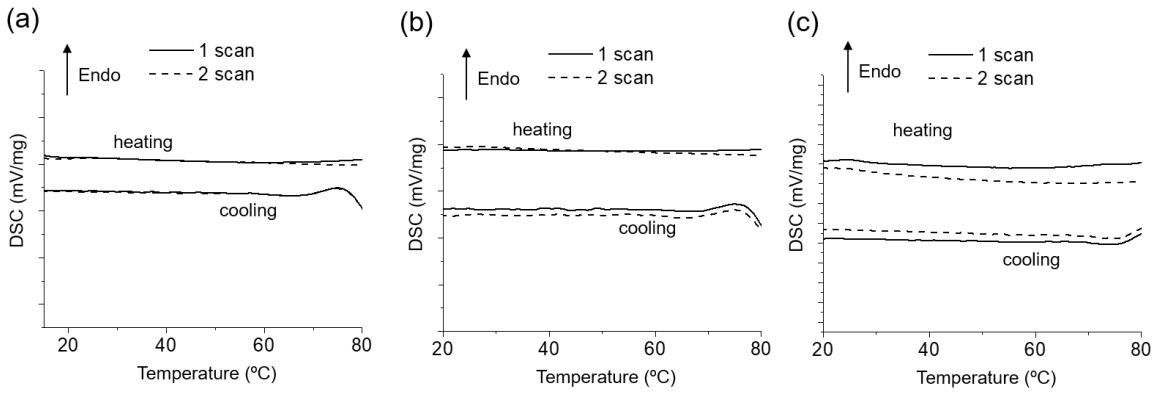

Figure S17. DSC profiles of (a) MPM-52, (b) MPM-78, and (c) MPM-92.

Temperature-dependent swelling behavior of MPMs. MPM hydrogels were fully swollen in water at 4 ºC and cut into a cylinder shape with a diameter of 25 mm and a thickness of 2 mm. These samples were soaked in the water between 4 ºC and 90 ºC, and their sizes after reaching the equilibria were recorded respectively.

PXRD measurements. PXRD experiments were performed on a Rigaku MiniFlex diffractometer. The voltage was set to 40 kV, and the current was 40 mA. The detector collected data over the range $2\theta = 5 – 45^{o}$. Solid-state samples of PM were prepared by lyophilizing the PM hydrogels. MPM-52, MPM-78 and MPM-92 were fully swollen at 4 or 20 ºC and then lyophilized to their powder form. MPM-52, MPM-78 and MPM-92 were heated to 90 ºC and naturally dried at 90 ºC in an open air for 48 h.

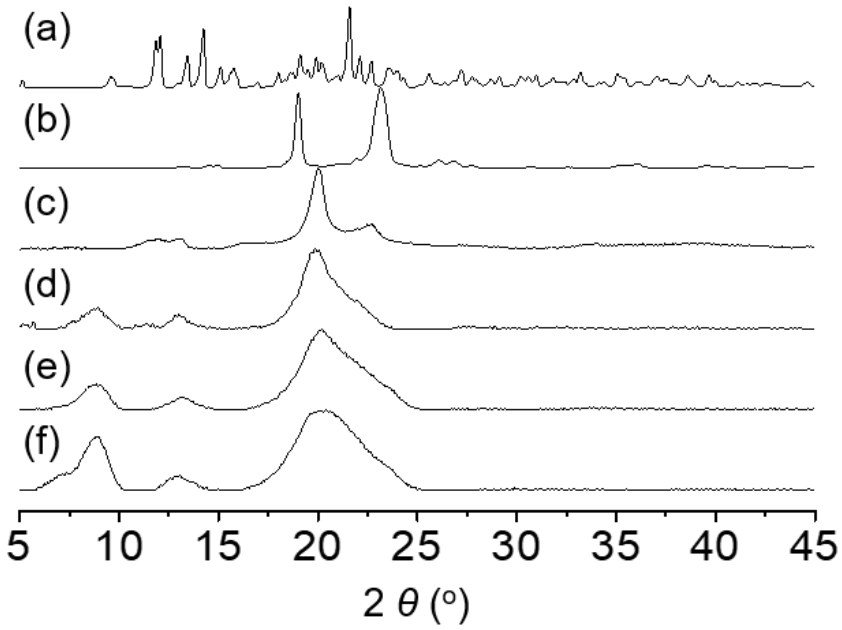

Figure S18. PXRD profiles of (a) α-CD, (b) PEG-20K, (c) lyophilized PM, (d) lyophilized MPM-52, (e) lyophilized MPM-78, (f) lyophilized MPM-92.

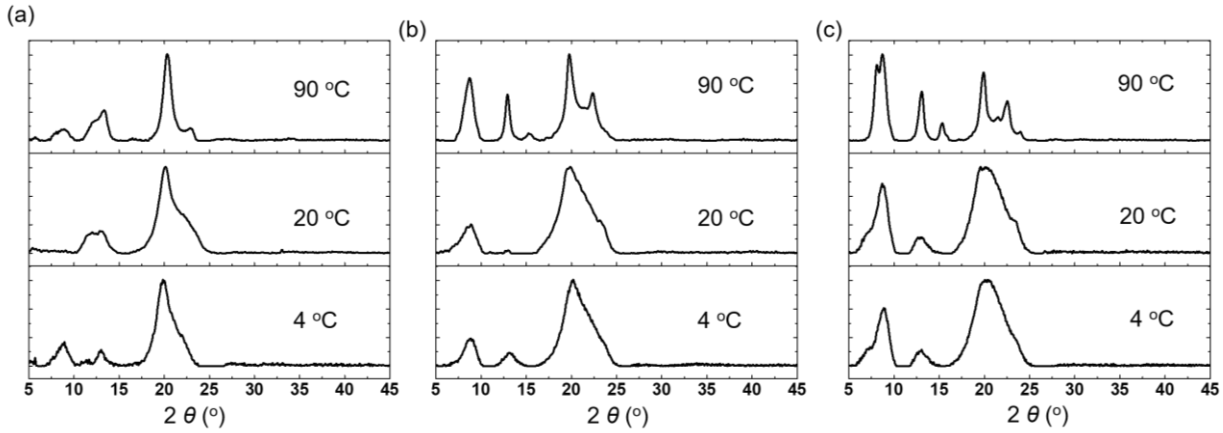

Figure S19. Powder X-ray diffraction profiles of MPM with a DS of (a) MPM-52, (b) MPM-78, and (c) MPM-92 prepared at 4 °C, 20 °C, and 90 °C, respectively.

The XRD spectra for MPM-92 at 4 ℃, 20 ℃ and 90 ℃ were deconvoluted with individual peak fitting by 'pseudo-Voigt' profile with 0.5 Lorentzian peak where K-alpha2 was considered. The background curve was fitted using 4th-order polynomial to afford better precision.

Note: The Pseudo-Voigt function is an approximation for the Voigt function, which is a convolution of Gaussian and Lorentzian function. It is often used as a peak profile in powder diffraction for cases where neither a pure Gaussian nor Lorentzian function appropriately describe a peak. Instead of convoluting those two functions, the Pseudo-Voigt function is the linear combination of Gaussian peak G(x) and a Lorentzian peak L(x), weighted by a fourth parameter (values between 0 and 1), which shifts the profile more towards pure Gaussian or pure Lorentzian when approaching 1 or 0 respectively, see the reference[3] for detailed justification for the peak fitting.

Grain size was calculated based on Scherrer equation:

$$\tau = \frac{K\lambda}{\beta \cos\theta}$$

τ is the mean size of the ordered domains;

K is the shape factor, where 0.9 was selected, assuming as an "overall average" shape factor;

λ is the wavelength of the diffractometer, where the value is 0.154 nm;

β is the FWHM of corresponding peak and was converted to radians for calculation;

θ is the Bragg angle.

The crystallinity of the polymer network was calculated using XRD deconvolution method, where the amorphous and crystalline contributions were separated. Then the peak area from crystalline

peak was selected as the crystalline fraction, the overall peak area was used as the $I_{overall}$ and $I_{overall}=I_A+I_C$, crystallinity= $I_C/I_{overall}$

Note: this is a rough estimation and can only be used as a qualitative comparison unless accurate calibration has been made.

MPM-92 at 4 ℃: residual error of fit 1.99 %, crystallinity = 19.38 % (numbers bracketed are errors associated with the peak information, peak marked as red is selected for crystallinity calculation)

Table S3. Peak deconvolution and fitting information for MPM-92 prepared at 4 °C

Residual Error of Fit = 1.99 %, total Area = 1300976 (6557), crystallinity = 19.38(0.15) %						
2θ	d (Å)	height	area	FWHM-θ	breadth	BG
8.995 (0.016)	9.8231 (0.0341)	2042 (12)	252167 (2697)	2.041 (0.023)	2.47	3673
12.967 (0.038)	6.8216 (0.0393)	1042 (12)	199217 (3409)	3.076 (0.052)	3.824	3080
20.031 (0.016)	4.4290 (0.0069)	2850 (8)	849597 (5031)	4.750 (0.032)	5.962	2389

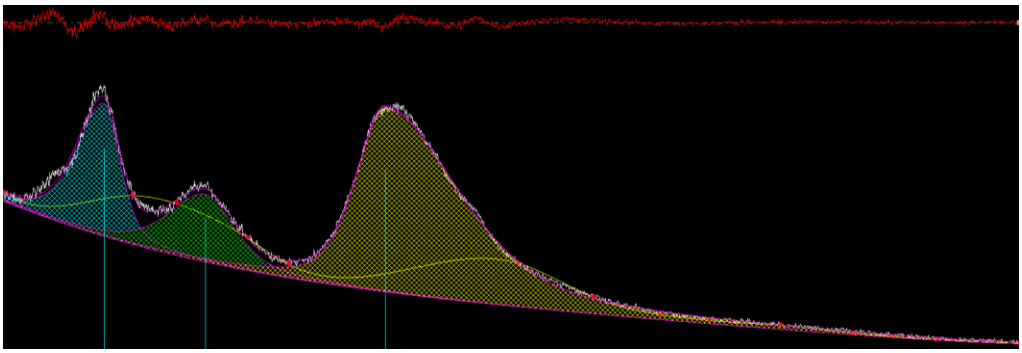

Figure S20. PXRD profile of MPM-92 prepared at 4 ℃ deconvoluted by 'pseudo-Voigt' profile for the peaks and 4th order polynomial for the background curve.

Table S4. Mean size of ordered domain for MPM-92 prepared by at 4 ℃ calculated by Scherrer equation.

2θ	FWHM	mean size of ordered domain (nm)
8.995	2.47	3.2
12.967	3.824	2.1
20.031	5.962	1.4

MPM-92 at 90 ℃: residual error of fit 3.52 %, crystallinity = 60.35 % (numbers bracketed are errors associated with the peak information, peak marked as red is selected for crystallinity)

Table S5. Peak deconvolution and fitting information for MPM-92 prepared at 90 ℃

Residual Error of Fit = 3.52 %, Total Area = 963074 (15603), Crystallinity = 60.35(2.09) %						
2θ	d (Å)	height	area	FWHM-θ	breadth	BG
8.056 (0.015)	10.9653 (0.0396)	1955 (131)	72892 (5438)	0.585 (0.039)	0.746	2721
8.729 (0.013)	10.1223 (0.0311)	2899 (36)	171886 (8229)	0.925 (0.056)	1.186	2524
13.033 (0.012)	6.7870 (0.0125)	1702 (17)	84951 (1093)	0.774 (0.010)	0.998	1658
15.402 (0.028)	5.7483 (0.0209)	607 (12)	35001 (1246)	0.904 (0.036)	1.153	1401
19.881 (0.011)	4.4621 (0.0051)	2042 (18)	105432 (1276)	0.797 (0.010)	1.033	1169
22.635 (0.023)	3.9250 (0.0079)	954 (8)	111007 (2080)	1.829 (0.040)	2.327	1116
23.001 (0.107)	3.8634 (0.0356)	622 (17)	381905 (11725)	10.541 (0.229)	12.28	1111

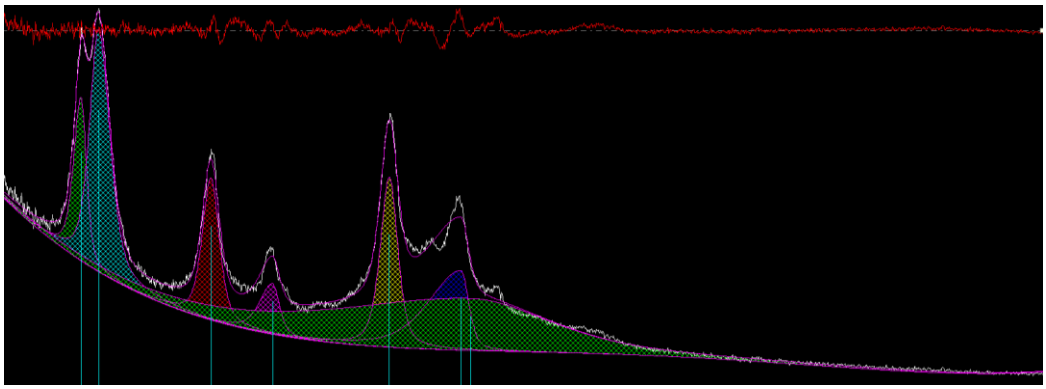

Figure S21. PXRD profile of MPM-92 prepared at 90 ℃ deconvoluted by 'pseudo-Voigt' profile for the peaks and 4th order polynomial for the background curve.

Table S6. Mean size of ordered domain for MPM-92 prepared by at 90 ℃ calculated by Scherrer equation.

2θ	FWHM	mean size of ordered domain (nm)	2θ	FWHM	mean size of ordered domain (nm)
8.056	0.585	13.6	15.402	0.904	8.9
8.729	0.925	8.6	19.881	0.797	10.1
13.033	0.774	10.3	22.635	1.829	4.4

S3. 3D Printing and Thermal Responsive Investigation.

Synthesis of the crosslinked Poly(*N*-isopropylacrylamide) (PNIPAM): Covalently crosslinked PNIPAM hydrogel was synthesized as a reference gel. An NIPAM aqueous solution (NIPAM: 1.13 g, 0.01 mol, solution: 1 M, 10 mL), *N*,*N* – methylenebisacrylamide (MBAA, 62 mg, 0.04 eq to NIPAM), and photo-initiator lithium phenyl-2,4,6-trimethylbenzoylphosphinate (LAP, 30 mg, 0.01 eq to NIPAM) were mixed together. The solution was transfer to a mold and photo-irradiated under UV light (365 nm) for 1 h. The crosslinked hydrogel was washed by an excess of water.

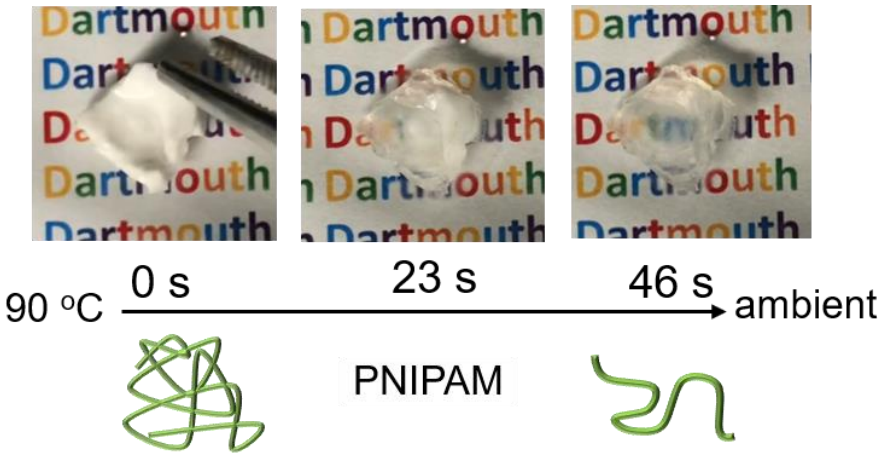

Figure S22. Opacity change of PNIPAM after removing the thin plate from a 90 °C heating chamber and placed it at ambient environment on a glass slide.

***3D Printing*.** The preparation of the native α-CD polypseudorotaxane 3D printing ink followed our reported method.[1,2] Briefly, the polypseudorotaxane hydrogel (PRH) was loaded in syringes equipped to the 3D printers (nScrypt or Cellink). The printing scripts was generated by CAD software. The printing speed varies between 5 – 40 mm/s. After printing, the monoliths were photo-crosslinked under UV light and washed by DMSO and water respectively.

***Shape morphing of 3D-printed sea star*.** A sea star monolith was printed using PRH as the ink. The sample was photo-crosslinked, washed and methylated using MeI (16 equiv. to -OH of PM's

CD). After methylation, the 3D-printed sea-star was stored in H_2O at 4 ºC. Then the sample was heated to 40 ºC and 90 ºC in H_2O, respectively.

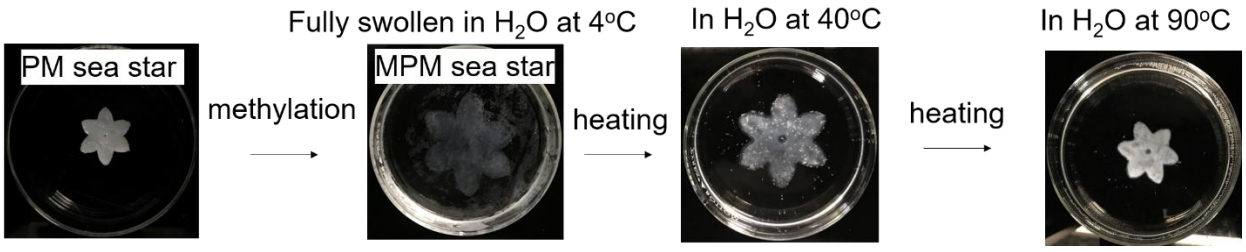

Figure S23. Images of a sea-star in its as-printed PM form, and methylated MPM form at different temperatures.

Preparation of DMA ink. Preparation of the ink was conducted following the method reported in previous literature.[4] Briefly, dimethylacrylamide (1 g, 0.01 mol) and the crosslinker MBAA (0.154 g, 0.001 mol) were dissolved in 10 mL H_2O with the 3D printing template Pluronic F127 (4.5 g) and DMPA's VP solution (60 % w/v, 43 µL, 0. 1 mmol DMPA) at 4 °C. The solution was stored at 4 °C overnight to remove air bubbles and it transformed to a hydrogel after being warmed to room temperature.

***Dual-Material 3D Printing*:** PRH and DMA inks were loaded into two syringe barrels respectively and installed to different printing heads on the 3D printer. The printing scripts were generated as shown below. The bottom layer was printed into crosshatch using DMA ink and the upper layer was printed into vertical or horizontal parallel patterns using PRH ink. The printed monoliths were photo-crosslinked under UV light (365 nm) for 2 h, followed by washing (DMSO and H_2O). These samples were methylated using MeI (16 equiv. to -OH of α-CDs).

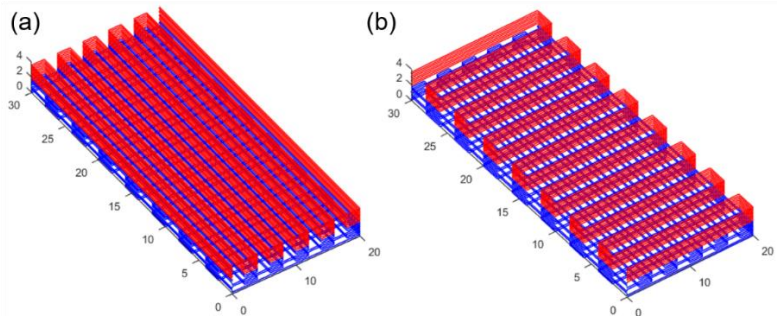

Figure S24. 3D-printing script of the hybrid with temperature-active precursor (PRH, upper layer, red) on temperature-passive layer (DMA ink, lower layer, blue), PRHs are printed in (a) vertical or (b) horizontal patterns.

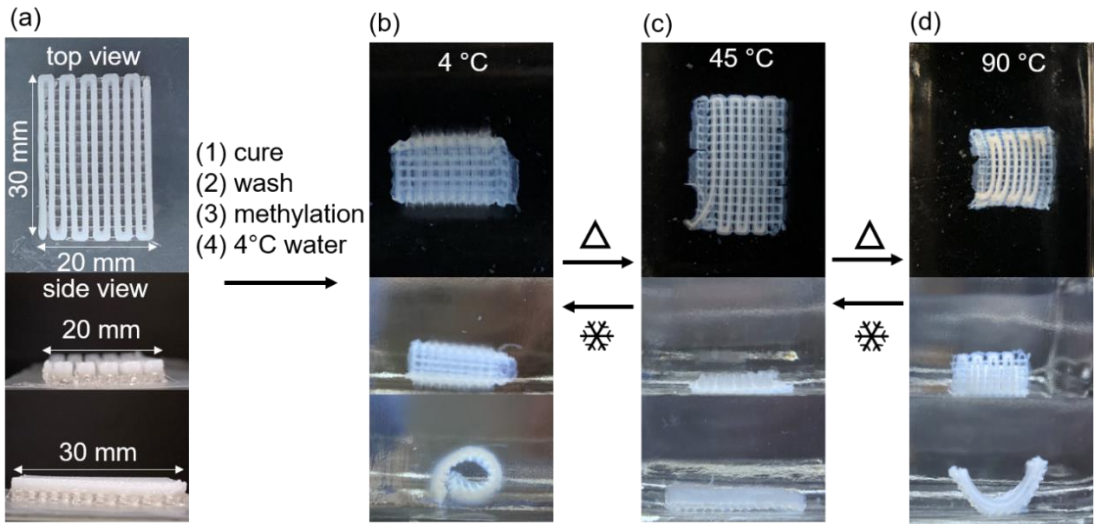

Figure S25. Temperature induced shape morphing of a bilayer monolith in its (a) as-printed state, (b) at 4 °C, (c) 45°C and (d) 90 °C, respectively. The top layer is constructed by MPM-92 (vertical pattern) and the bottom layer is constructed by crosslinked PDMA.

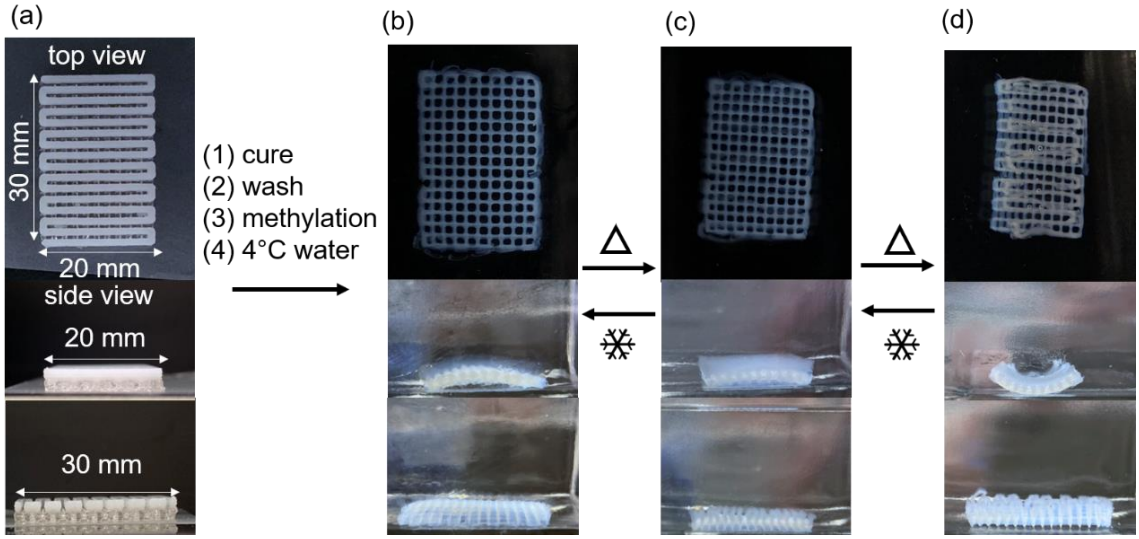

Figure S26. Temperature induced shape morphing of a bilayer monolith in its (a) as-printed state, (b) at 4 °C, (c) 45°C and (d) 90 °C, respectively. The top layer is constructed by MPM-92 (horizontal pattern) and the bottom layer is constructed by crosslinked PDMA.

S4. References

(1) Lin, Q.; Hou, X.; Ke, C. Ring Shuttling Controls Macroscopic Motion in a Three-Dimensional Printed Polyrotaxane Monolith. *Angew. Chem. Int. Ed.* **2017**, *56*, 4452–4457..

(2) Lin, Q.; Li, L.; Tang, M.; Hou, X.; Ke, C. Rapid Macroscale Shape Morphing of 3D-Printed Polyrotaxane Monoliths Amplified from PH-Controlled Nanoscale Ring Motions. *J. Mater. Chem. C* **2018**, *6*, 11956–11960.
(3) Enzo, S.; Fagherazzi, G.; Benedetti, A.; Polizzi, S. A Profile-Fitting Procedure for Analysis of Broadened X-Ray Diffraction Peaks. I. Methodology. *J. Appl. Crystallogr.* **1988**, *21*, 536–542.
(4) Li, L.; Zhang, P.; Zhang, Z.; Lin, Q.; Wu, Y.; Cheng, A.; Lin, Y.; Thompson, C. M.; Smaldone, R. A.; Ke, C. Hierarchical Co-Assembly Enhanced Direct Ink Writing. *Angew. Chem.* **2018**, *130*, 5199–5203.